MoDE: Mixture of Diffusion Experts for Any Occluded Face Recognition

Qiannan Fan[1,2], Zhuoyang Li[2], Jitong Li[2†], Chenyang Cao[2*]
[1]State Grid Tianjin Economic Research Institute, Tianjin, China
[2]College of Intelligence and Computing, Tianjin University, Tianjin, China
qiannanfan@outlook.com, 2125867922@qq.com, jitong_li@yeah.net, 1035363213@qq.com

arXiv:2505.04306v1 [cs.CV] 7 May 2025

***Abstract*—With the continuous impact of epidemics, people have become accustomed to wearing masks. However, most current occluded face recognition (OFR) algorithms lack prior knowledge of occlusions, resulting in poor performance when dealing with occluded faces of varying types and severity in reality. Recognizing occluded faces is still a significant challenge, which greatly affects the convenience of people's daily lives. In this paper, we propose an identity-gated mixture of diffusion experts (MoDE) for OFR. Each diffusion-based generative expert estimates one possible complete image for occluded faces. Considering the random sampling process of the diffusion model, which introduces inevitable differences and variations between the inpainted faces and the real ones. To ensemble effective information from multi-reconstructed faces, we introduce an identity-gating network to evaluate the contribution of each reconstructed face to the identity and adaptively integrate the predictions in the decision space. Moreover, our MoDE is a plug-and-play module for most existing face recognition models. Extensive experiments on three public face datasets and two datasets in the wild validate our advanced performance for various occlusions in comparison with the competing methods.**

***Index Terms*—occluded face recognition, generative model, diffusion expert**

I. Introduction

Face recognition is ubiquitous and has been widely applied in various applications [1], such as security, payment, and social media. Recent face recognition algorithms [2], [3], such as FaceNet [4], [5], CosFace [6], and ArcFace [7], have shown remarkable performance in unobstructed face recognition. However, many practical scenarios may cause the face to be obscured. In particular, the frequent flu epidemics have led to more people getting used to wearing masks to protect themselves and others, bringing new challenges to face recognition, which significantly impacts the convenience of daily security. Moreover, the uncertainty of occluded face regions and the diversity of occlusion types (*e.g.*, accessories, glasses, hats, and masks) require more robust and generalized face recognition techniques [8]. The occluded face parts usually result in discriminative information loss and feature changes, leading to a significant decline in the recognition accuracy of most traditional face recognition models.

In recent years, some studies have emerged to improve occluded face recognition accuracy. These methods can be mainly grouped into three categories [9]. i) Occlusion robust feature extraction (ORFE) aims to extract features that are less affected by occlusions, such as Local Binary Patterns (LBP) [10], [11] and Elastic Bunch Graph Matching (EBGM) [12]. However, most of these methods rely on handcrafted features and require prior knowledge, which limits their effectiveness. ii) Occlusion-aware face recognition (OAFR) discards occluded parts and only uses visible face parts that qualify for face recognition. This approach requires detecting the occluded parts, which can be challenging in the case of irregular occlusions. iii) Occlusion recovery-based face recognition (ORecFR) uses a reconstruction model to repair occluded faces for the demands of conventional face recognition systems. However, these models may not generalize well to occlusions that are not present in the training set, which could result in unsatisfied results [13]. Furthermore, while the reconstructed images may present visually convincing, they might be tangled in poor authenticity and identity ambiguity.

Fig. 1: To demonstrate the adaptability of our method for multi-occluded face recognition, we visualize some face images from the LFW dataset with six different face occlusions, each image is repainted below. The right part shows the accuracy comparison between the baseline and our method.

In this paper, we propose an identity-gated mixture of diffusion experts (MoDE) framework for occluded face recognition. By integrating multiple diffusion experts, we obtain identity-preserving reconstructed face images while improving recognition accuracy. Specifically, the MoDE utilizes diffusion experts to generate reconstructed images for each occluded face, regardless of the type of occlusions. The diffusion model endows diverse potential visual appearances for the repaint results that provide both effective and redundant information for identification. To fully exploit the identity information from various reconstructed images, we further design an identity

†Work done during internship at Tianjin University.
*Corresponding author.

gating (ID-Gate) network that estimates the authenticity of multiple input images and outputs the corresponding contribution to the identification of the similarity matrix. To this end, MoDE exhibits excellent performance for multiple occluded face recognition, Fig. 1 illustrates it. Furthermore, the adaptively selected results of MoDE serve as valuable references for evaluating the identity consistency of the reconstructed images. We have performed experiments on various datasets to demonstrate the superiority against competing methods. Our main contributions can be summarized in three aspects:

1) We propose a dynamic occluded face recognition framework, which integrates multiple generative experts in the decision space through ID-Gate and subtly leverages comprehensive identity information produced by them.
2) We introduce the diffusion model to reconstruct occluded faces with high image quality and diversity. Our approach is capable of identifying various types of occlusions, even in extreme conditions. To our knowledge, our work is the first to introduce the diffusion model to occluded face recognition.
3) Our MoDE is a flexible *plug-and-play* module that can be seamlessly combined with most existing face recognition models and achieve stable improvements. Extensive experiments validate our superiority.

II. Related Works

General Face Recognition have achieved impressive results and have focused primarily on designing novel network architectures [14], [15] and loss functions [16], [17]. The early models relied on multiple deep convolutional neural networks to extract facial features, which were later fused together [18], [19]. However, the use of a single network to extract features has now dominated mainly [4]. Meanwhile, the softmax loss for multiclass classification is widely used and significantly boosted by angle-based techniques [6], [7], [20].

Occluded Face Recognition has become a persistent challenge in computer vision [9]. Existing methods can be broadly categorized into robust occlusion feature extraction (ORFE), occlusion-aware face recognition (OAFR), and occlusion-recovery-based face recognition (ORecFR). ORFE aims to extract features from an image or video that are robust to occlusions [10], [11], [21]. However, the accuracy of these methods is limited by the limited discriminability of feature representation [22]. OAFR uses visible facial parts alone for recognition to alleviate the occlusion effect [23]–[25]. They mainly exploit limited information from partial faces. ORecFR [26] recovers the occlusion with non-blind or blind inpainting. With novel occlusions, these models often illustrate inadequate reconstruction and recognition capabilities.

Image Repainting aims to fill in the gaps and missing components of an image. Generative Adversarial Nets (GANs) [27], such as AttGAN [28], ID-GAN [29] have been widely used in various image generation applications [30]. However, many GAN-based image reconstruction methods [31] often produce deterministic transformations, leading to poor diversity in generated images [32], and the restored results may appear seriously ambiguous or blurry [33]. Recently, Diffusion models have gained popularity for their powerful generative capacity to capture complex data distributions and model the underlying dynamics of image generation processes [34]–[36]. Ho et al. [37] introduced a new SDE-based generative model, Denoising Diffusion Probabilistic models (DDPMs), which employed an incremental generative process to efficiently generate data and capture complex data distributions. In this paper, we employ the diffusion model to repaint occluded faces, empowering a significant diversity of potential occluded facial components and assembling them for face recognition.

III. Methodology

A. Face Repainting

We employ a Denoising Diffusion Probabilistic Model [37] in our face repainting framework, as shown in Fig. 2. It iteratively denoises a random noise sample x_T until a high-fidelity output image x_0^d is obtained. During the diffusion process, the initial image x_0^d diffuses to white Gaussian noise x_T over a duration of T time steps.$q\left(x_t \mid x_{t-1}\right)$ represents the probability distribution of the current image given the previous image at step t:

$$q\left(x_t \mid x_{t-1}\right)=\mathcal{N}\left(x_t ; \sqrt{1-\beta_t} x_{t-1}, \beta_t \mathbf{I}\right). \tag{1}$$

At each step, Gaussian noise with variance β_t is added to the previous image x_{t-1}, preserving $\sqrt{1-\beta_t}$ of it, where $\mathbf{I}$ is the identity matrix. By defining $\bar{\alpha}_t=\prod_{s=1}^t\left(1-\beta_s\right)$, we can thus rewrite 1, as a single step:

$$q\left(x_t \mid x_0^d\right)=\mathcal{N}\left(x_t ; \sqrt{\bar{\alpha}_t} x_0^d,\left(1-\bar{\alpha}_t\right) \mathbf{I}\right). \tag{2}$$

For the denoising process, the model predicts the noise ϵ_θ that is added to x_t during the diffusion process, and then subtracts this noise from x_{t-1} to obtain a cleaner image as,

$$p_\theta\left(x_{t-1} \mid x_t\right)=\mathcal{N}\left(x_{t-1} ; \mu_\theta\left(x_t, t\right), \Sigma_\theta\left(x_t, t\right)\right), \tag{3}$$

where $\mu_\theta\left(x_t, t\right)$ and $\Sigma_\theta\left(x_t, t\right)$ are the parameters of the Gaussian distribution.

As shown in Fig 3, the repainting model is improved in the denoising process by dividing x_{t-1} into two parts: $m \odot x_{t-1}^{known}$, consisting of real images, and $(1-m) \odot x_{t-1}^{unknown}$, consisting of denoising results from x_t.

$$x_{t-1}=m \odot x_{t-1}^{known}+(1-m) \odot x_{t-1}^{unknown}, \tag{4}$$

$$x_{t-1}^{known} \sim \mathcal{N}\left(\sqrt{\bar{\alpha}_t} x_0^d,\left(1-\bar{\alpha}_t\right) \mathbf{I}\right), \tag{5}$$

$$x_{t-1}^{unknown} \sim \mathcal{N}\left(\mu_\theta\left(x_t, t\right), \Sigma_\theta\left(x_t, t\right)\right), \tag{6}$$

where m is a mask matrix with elements in $[0,1]$, $\odot$ denotes element-wise multiplication, x_{t-1}^{known} is sampled using the known pixels in the given images, while $x_{t-1}^{unknown}$ is sampled from the model, given the previous iteration x_t. This approach ensures that at each denoising iteration, x_t is determined solely by x_{t-1}, and the distribution of the original image x_0^d is incrementally incorporated in each iteration.

Although, it effectively enhances the quality of the output image, there will be a problem of boundary discontinuity

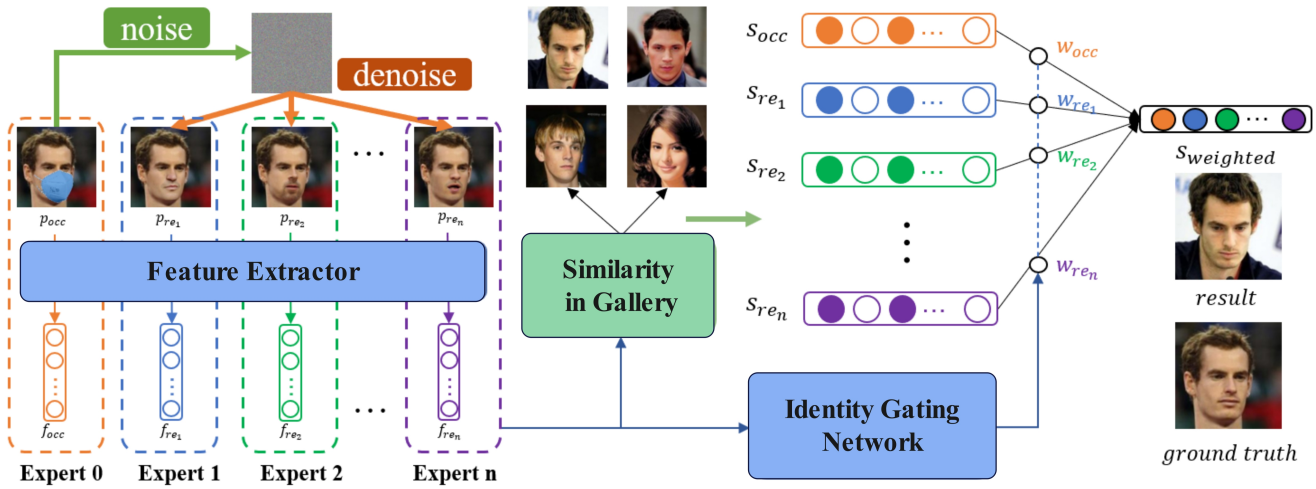

Fig. 2: The framework of our MoDE. Firstly, MoDE reconstructs the occluded image and produces n repainted images. Then, it extracts the features from the repainted images and the original occluded image, which are then inputted into ID-Gate to output the weight vector. Finally, we calculate the similarity matrix of each image and multiply it with the weight vector to generate a weighted similarity matrix, thereby obtaining the recognition result.

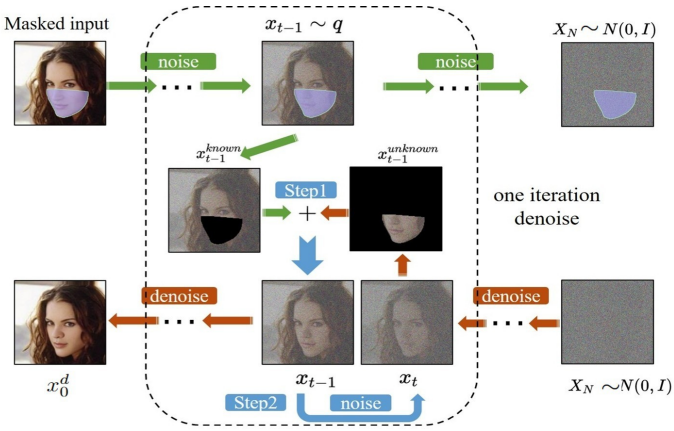

Fig. 3: Face Repainting. Repaint modifies the standard denoising process to condition on the given image content. In each step, it samples the known region (top) from the input and the repainted part from the output (bottom).

during the stitching process. To solve this problem, a j iterative resampling step is added to the x_t and x_{t-1} steps, so that the boundaries in the output image are aligned consistently.

The framework, illustrated in Fig. 3, involves an iterative denoising method for repainting an occluded face image. Each iteration consists of two steps: Firstly, we synthesize and splice x_{t-1} by combining the known and unknown parts using formulas 4, 5, and 6. Secondly, we resample x_{t-1} by adding noise to obtain x_t. We perform the two steps r times for one denoising iteration, which differs from previous work by incorporating resampling to improve the boundary, since face images have complex boundaries, and simple synthesis methods can create unnatural transitions and artifacts. By adding a resampling step and introducing noise, the model can better mimic the randomness in natural images, enhancing boundary smoothness.

B. ID-Gated MoDE

1) Identity Gating Network: To effectively assemble information from multiple reconstructed facial images, we introduce an identity gating network (ID-Gate) [38] for evaluating the individual contributions of each reconstruction to the identity, and adaptively integrating the predicted results in the decision space. The ID-Gate takes a set of facial features extracted from the occluded image and repainted images as input, and produces a weight vector for each image in the decision space as output.

Specifically, for a sequence of facial images denoted as $X = [x_0, x_1, \ldots, x_n]$, the extracted features are represented as $F(X) = [f(x_0), f(x_1), \ldots, f(x_n)]$, which are then fed into the ID-Gate. The weight vector, denoted as $W(X)$, is utilized to integrate the predicted results of the facial images within the decision space, and is calculated as:

$$W(X) = softmax(W_g \cdot F(X) + b_g), \tag{7}$$

This computes the weights for fusing experts' predictions via ID-Gate. where W_g and b_g are trainable parameters.

It is imperative to highlight that the ID-Gate distinguishes itself from the gating network employed in the typical Mixture of Experts models on the following grounds:

Network input/output: Most gating networks take a single feature as input, making them a single-input network, and output weights for the features of different expert networks. However, Our ID-Gate receives features from multiple experts

as inputs, making it a multi-input network, and produces weights for predictions. It endows each expert with specific knowledge for the corresponding face repainting diffusion model.

Network objective: The objective of most gating networks in the typical Mixture of Experts model aims to fuse features within the feature space. While our ID-Gate is designed to integrate identity prediction results based on deep representation features, thereby implicitly comparing the reconstructed results with the original occluded faces for more effective, interpretable, and intuitive decision fusion.

2) Mixture of Diffusion Experts: Based on face repainting and the ID-Gate, we propose a novel identification framework, called Mixture of Diffusion Experts (MoDE). It consists of $n+1$ "experts", denoted as $E_0, E_1, \ldots, E_n$, along with the ID-Gate, as depicted in Fig. 2. Within each expert, the repainted face and the feature extraction network are employed to generate the feature vectors of the experts. The feature extraction network within each expert shares parameters to ensure consistency. In order to retain the identity information of the image, we designate E_0's image as the original image with occlusion, denoted as x_0. As the diffusion model serves as the foundation for face repainting in our work, each "expert" is taken as a diffusion expert.

Given the input x_0, the repaint process generates a sequence of images for each expert, denoted as $X = [x_0, x_1, \ldots, x_n]$. Subsequently, the feature extraction network is employed to obtain the feature output $f(x_i)$ of the experts. The similarity matrix $s(x_i)$, calculated based on the features, is used to represent the prediction results of the faces in the gallery, and the features are also fed into the ID-Gate to generate the weight vector $w(x_i)$ for integrating the predictions in the decision space. Finally, the Mixture step is performed, where the results of the diffusion experts are integrated using the weight vector.

$$S_X = \sum_{i=0}^{n} w(x_i) s(x_i). \tag{8}$$

By applying the argmax function on the weighted similarity matrix S_X, the best matching face can be identified.

C. Objective Loss

In MoDE, the overall objective loss is decomposed into two components: the loss incurred during the pre-training of the diffusion model and the training loss of ID-Gate. During the training of the diffusion model, the loss function is optimized through the minimization of the negative log-likelihood of the model in training set, which can be mathematically expressed as:

$$\mathcal{L}_{simple} = E_{t, x_0^d, \epsilon}\left[\left\|\epsilon - \epsilon_\theta\left(x_t, t\right)\right\|^2\right], \tag{9}$$

where $\mathcal{L}_{simple}$ represents the loss function, $\epsilon_\theta\left(x_t, t\right)$ represents a learned denoising diffusion process, and $\|\cdot\|$ represents a Euclidean distance metric. The expectation over t, x_0^d, ϵ ensures robust denoising of occluded inputs under varying timesteps and noise. Moreover, $\mu_\theta\left(x_t, t\right)$ defines the mean of the latent variables of the diffusion model as:

$$\mu_\theta\left(x_t, t\right) = \frac{1}{\sqrt{\alpha_t}}\left(x_t - \frac{\beta_t}{\sqrt{1-\bar{\alpha}_t}}\epsilon_\theta\left(x_t, t\right)\right). \tag{10}$$

The ID-Gate is optimized by the cross-entropy loss:

$$\begin{aligned}\mathcal{L} &= \frac{1}{B}\sum_{k=1}^{B} l(S_{X_k}, label_k) \\ &= -\frac{1}{B}\sum_{k=1}^{B} log(\frac{\exp(S_{X_k}[label_k])}{\sum_{i=1}^{M}\exp(S_{X_k}[i])}),\end{aligned} \tag{11}$$

where B and S_{X_k} are the batch size and weighted similarity matrix of the k-th identity, M denotes the total number of identities, and $label_k$ is the label of the k-th identity.

D. Network Architecture

The ID-Gate in MoDE can be one of the following two network architectures.

Softmax Gating: A straightforward choice of gating network [39] involves multiplying the input by a trainable weight matrix W_g, adding the bias b_g, and then applying the Softmax function.

Noisy Top-K Gating: The Softmax gating network can be augmented with two components: sparsity [40] and noise. Before applying the Softmax function, tunable Gaussian noise is injected through the $StandardNormal()$ term which adds i.i.d. Gaussian noise $\epsilon_i \sim \mathcal{N}(0,1)$ into each gating component, encouraging exploration during training. Only the top k values are retained, with the rest set to $-\infty$. The sparsity improves computation efficiency. The amount of noise per component is controlled by a second trainable weight matrix W_{noise},

$$G(x) = Softmax(K - TopK(H(x), k)), \tag{12}$$

$$H(x)_i = \left(x \cdot W_g\right)_i + StandardNormal() \cdot Softplus\left(\left(W_{noise} \cdot x\right)_i\right), \tag{13}$$

$$K{-}TopK(v,k)_i = \begin{cases} v_i & \text{if } v_i \text{ is in the top } k \text{ elements of } v. \\ -\infty & \text{otherwise.} \end{cases} \tag{14}$$

For ID-Gate, we use the first Softmax Gating, and the second Noisy Top-K Gating is discussed in the appendix.

IV. Experiments

We first compare our method with five state-of-the-art face recognition methods, including ArcFace [7], FaceNet [4], [5], CosFace [6], FFR-Net [41], and Deepface-EMD [42]. Then, we validate the MoDE on two real datasets collected by ourselves: the Occluded Volunteer Face (OVF) dataset and the Web Wild Occluded Celebrity Face (WWCF) dataset.

A. Experimental Setting

Datasets: We conducted experiments on three datasets: MS1M [7], LFW [43] and CelebA [44]. MS1M consists of over one million face images from 13,126 different identities, LFW consists of 13,233 face images from 5,749 identities, while CelebA contains 202,599 face images from 10,177 different identities.

To simulate mask occlusion scenarios, we used facial keypoint detection to add mask textures to the face images in these datasets, creating three new sub-datasets: Occ MS1M, Occ LFW, and Occ CelebA. During the training phase, we selected 500 faces in the Occ MS1M dataset as the probe, and 2500 faces in MS1M as the gallery. During the testing phase, we randomly selected 500 faces in Occ MS1M, 1000 faces in Occ LFW and 1000 faces in Occ CelebA as the probe, respectively. We used 2500 faces in MS1M, 4000 faces in LFW and 5000 faces in CelebA as the gallery, respectively.

Evaluation Metrics: Our MoDE model was evaluated using four widely used evaluation metrics: $Top1$, $Top5$, EER, and Acc. $Top1$ and $Top5$ refer to the Top-1 and Top-5 face recognition accuracy rates respectively. For face verification, EER (Equal Error Rate) is a well-established metric in biometric verification systems and represents the point at which the FAR (False Acceptance Rate) and FRR (False Rejection Rate) are equal. Acc indicates the model's verification accuracy at the EER threshold.

Implementation Details: For image preprocessing, we first performed face detection on the images and then cropped and resized them to 112×112 pixels. To prevent overfitting and improve the generalization ability of our model, we applied data augmentation when training the Gate network. The input of the Gate network was a feature vector concatenated from $n+1$ feature vectors. We used the Adam optimizer with a learning rate of 1e-6, a batch size of 32, and trained for 200 epochs. For the repaint model, we set time steps $T = 200$, resampling times $r = 10$, and jumpy size $j = 10$. In the ablation study, we adopted the ResNet-50 convolutional neural network used by ArcFace [7] and pretrained on the MS1M dataset for feature extraction.

Competing Methods: ArcFace [7] is a deep face recognition method that improves the discriminability of face features by adding an angular margin to the feature space. It enhances the intra-class compactness and inter-class differences by increasing the normalization of the feature vector. FaceNet [4] is a convolutional neural network-based models that maps face images to a low-dimensional vector space, known as face embedding. It determines whether two face images belong to the same person by comparing their embedding vectors. CosFace [6] uses a margin-based softmax loss function similar to Sphereface [20] to constrain the weight matrix W in the classifier to a hypersphere, resulting in greater cosine similarity of face features for the same person and less cosine similarity between different people. FFR-Net [41] uses an encoder-decoder structure to map the occluded region features to the unoccluded region, thus improving the accuracy of face recognition. Deepface-EMD [42] is a re-ranking approach that compares two faces using the Earth Mover's Distance on the deep, spatial features of image patches.

B. Comparisons

To evaluate the effectiveness of our proposed method (MoDE), in comparison with existing mainstream face recognition techniques under occlusion, we evaluated five competing algorithms on three artificial occluded datasets: MS1M, LFW, and CelebA, and two real occluded datasets: OVF and WWCF.

TABLE I: Comparison between state-of-the-art models and MoDE in face recognition tasks on occluded MS1M, LFW and CelebA datasets. Our MoDE outperforms all other methods.

Dataset	Model	Method	Top1	Top5
Occ MS1M	ArcFace	baseline	87.8	93.6
		MoDE	88.8(+1.0)	95.0(+1.4)
	FaceNet	baseline	30.6	47.4
		MoDE	31.6(+0.2)	49.0(+1.6)
	CosFace	baseline	42.4	59.0
		MoDE	47.2(+4.8)	63.2(+4.2)
	FFR-Net	baseline	70.6	83.4
		MoDE	74.2(+3.6)	84.2(+0.8)
	DeepFace-EMD	baseline	18.6	32.6
		EMD	25.6(+7.0)	39.0(+6.4)
		MoDE	31.2(+12.6)	48.8(+16.2)
		EMD+MoDE	38.2(+19.6)	54.3(+21.7)
Occ LFW	ArcFace	baseline	64.6	79.3
		MoDE	71.4(+6.8)	82.0(+2.7)
	FaceNet	baseline	27.6	51.4
		MoDE	34.2(+6.6)	56.7(+5.3)
	CosFace	baseline	10.4	18.4
		MoDE	14.4(+4.0)	24.0(+5.6)
	FFR-Net	baseline	46.7	62.6
		MoDE	52.5(+5.8)	67.6(+5.0)
	DeepFace-EMD	baseline	22.2	40.2
		EMD	30.2(+8.0)	48.5(+8.3)
		MoDE	35.9(+13.7)	55.2(+15)
		EMD+MoDE	47.5(+25.3)	63.9(+23.7)
Occ CelebA	ArcFace	baseline	23.2	38.4
		MoDE	31.9(+8.7)	46.0(+7.6)
	FaceNet	baseline	16.4	31.0
		MoDE	21.5(+5.1)	37.4(+6.4)
	CosFace	baseline	3.4	9.7
		MoDE	9.6(+6.2)	17.0(+7.3)
	FFR-Net	baseline	15.0	26.0
		MoDE	20.2(+5.2)	32.5(+6.5)
	DeepFace-EMD	baseline	24.6	42.0
		EMD	32.2(+7.6)	48.0(+6.0)
		MoDE	31.6(+7.0)	50.2(+8.2)
		EMD+MoDE	37.3(+12.7)	54.3(+12.3)

1) Results on Artificial Occluded Face: Table I shows that MoDE outperforms all the competing methods in terms of recognition accuracy. Notably, we observed a significant increase in accuracy on the Occ LFW and Occ CelebA datasets compared to the Occ MS1M dataset.

FaceNet, ArcFace, and CosFace are feature extractors based on metric learning, aiming to increase intra-class compactness and inter-class separability. However, due to the absence of large-scale occluded face data for training, they are still affected by occlusion, resulting in a decline in recognition accuracy. FFR-Net is a method that focuses on converting occluded face features into unoccluded face features. However, its performance in real-world scenarios is not ideal, and it may

TABLE II: Comparisons in real scene.

Model	Method	OVF		WWCF	
		Top1	Top5	Top1	Top5
ArcFace	baseline	89.8	100	22.0	36.7
	MoDE	95.5	100	22.5	37.0
FaceNet	baseline	64.8	86.4	8.6	21.3
	MoDE	65.9	86.4	7.6	22.0
CosFace	baseline	83.0	96.6	4.1	8.7
	MoDE	93.2	100	5.3	10.8
FFR-Net	baseline	96.6	100	9.6	22.3
	MoDE	98.9	100	12.3	25.3
Deepface-EMD	baseline	69.3	93.2	16.4	31.7
	EMD	90.9	98.9	19.7	34.4
	MoDE	87.5	98.9	21.2	39.4
	EMD + MoDE	95.5	98.9	24.9	41.6

not be capable of handling occluded faces well. Deepface-EMD uses Earth Mover's Distance to add additional comparison stages to explicitly check image similarity at a fine-grained level. Similarly, MoDE is also a plug-and-play module that can be widely applied to any traditional face recognition model, achieving higher recognition accuracy than Deepface-EMD on Occ MS1M and Occ LFW. Moreover, we find the largest improvement when using both MoDE and Deepface-EMD, indicating that the two modules do not conflict.

Our proposed MoDE method addresses the occlusion problem by using a repaint model to generate high-quality reconstructions of occluded faces, and leveraging the ID-Gate module to selectively use input images with reliable identity information. Jointly using original and reconstructed image information produces superior performance in recognizing occluded faces. Hence, MoDE has inherent advantages in dealing with occlusion and could be considered a promising approach for occluded face recognition.

2) Results on Real Occluded Face: We evaluated the effectiveness of our proposed method in addressing occlusion challenges in real-world scenarios by collecting two occluded-face datasets and conducting experiments on them. The first, called the Occluded Volunteer Face Dataset (OVF), was obtained from volunteers wearing masks captured in various public settings, containing 352 face images of 44 identities. The second one, called the Web Wild Occluded Celebrity Face (WWCF) dataset, was collected from publicly available web images, including 873 face images from 233 identities.

As shown in Table II, MoDE performs better in dealing with face occlusion problems compared with most face recognition models. In contrast to artificial occluded datasets, real occluded datasets present greater challenges in face recognition tasks, due to the greater variability in occlusion location and degree, as well as the unpredictability of occlusion quality and shape. Fortunately, the repaint process of MoDE effectively resolves these issues by restoring features in occluded areas to the greatest extent possible. The ID-Gate module's adaptive selection mechanism guarantees the quality and credibility

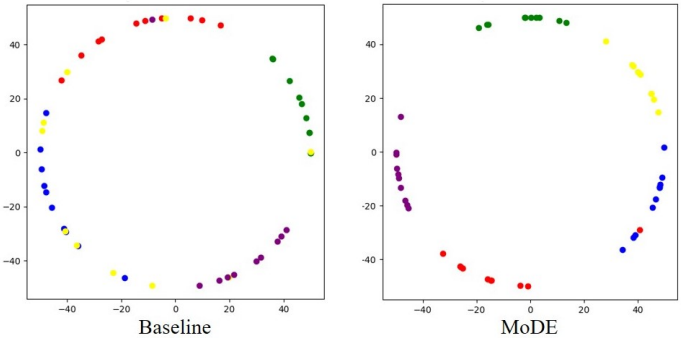

Fig. 4: Visualization of similarity distributions with t-SNE [45] and following normalization. Different markers with colors represent different classes.

TABLE III: Comparisons of three variants on Occ CelebA.

Method	Top1	Top5	Acc	EER
Baseline	23.2	38.4	83.5	0.165
Baseline + RF	28.7(+5.5)	41.1(+2.7)	85.6(+2.1)	0.145(-0.020)
MoDE	31.9(+8.7)	46.0(+7.6)	85.4(+1.9)	0.146(-0.019)

of input data, enabling more efficient utilization of identity information. Moreover, it is noteworthy that MoDE has demonstrated remarkable performance on small-scale datasets when incorporated with specific methodologies (FFR-Net, OVF, 98.9%), indicating its potential practical utility.

C. Ablation Study

We performed ablation studies as follows:

(1) **Baseline**: ResNet-50 was served as the feature extractor for occluded face recognition directly.
(2) **Baseline + RF**: Diffusion experts were introduced to generate multiple repainted faces (RF), which were subsequently fused by averaging.
(3) **MoDE**: We utilized ID-Gate to adaptively integrate the predictions of occluded faces and multiple repainted faces in the decision space.

Quantitative Results: Table III presents the results of various experimental variants on the Occ CelebA dataset. Among all the variants, the MoDE model achieved the highest recognition Top-1 and Top-5 accuracy, with an 8.7% and 7.6% improvement over the "Baseline" Top-1 and Top-5 accuracy, respectively. Leveraging the diverse identity information obtained from repainted images, the "Baseline + RF" approach achieved a certain level of improvement. However, it viewed all repainted images as equal and ignored the diversity of the diffusion model, failing to adaptively differentiate between relevant and redundant information for identification. In contrast, the incorporation of ID-Gate allowed for dynamic decision space integration of multiple experts to filter out noise from repainted images that failed to meet our expectations, thereby enhancing the model's adaptability and fault tolerance.

Qualitative Analyses: To evaluate the effectiveness of MoDE in occluded face classification, we compared the similarity distributions of the baseline and MoDE on a subset of the Occ MS1M dataset. We randomly selected five classes, each

Fig. 5: Visualization of face repaint error. The first three columns represent normal faces, occluded faces and repainted faces, respectively. The last three columns represent heatmaps indicating the degree of information loss between GT and Occluded, RF, and MoDE, respectively.

with 10 samples, and used a gallery with 500 identities. Then we obtained the 500-dimensional similarity distribution for each model and transformed the features into 2D using t-SNE. The normalized results are depicted in Fig. 4. The similarity distribution of the baseline model is scattered, indicative of subpar performance in occluded face classification. In contrast, MoDE's similarity distribution is more compact and distinguishable, highlighting its outstanding capability to address occlusion challenges. This is credited to its deep representation features obtained through decision space integration.

To investigate the benefits of the MoDE method in detail, we compared the heat maps of information loss identified when using occluded images, repainted images, and the MoDE method. As illustrated in Fig. 5, a larger area and more intense color on the heatmap indicate a more substantial loss of information. Occluded images result in complete loss of information in the occluded regions (as seen by the area and color of the heat map). Repainted images may alleviate the problem, but significant loss still remains in some regions. In contrast, the MoDE method yielded the best results, emphasizing its superior capability in both minimizing information loss and maximizing identity utilization for recognition.

D. Discussion

Hyperparameter Analysis: We conducted a hyperparameter analysis to determine the optimal value of n that indicates the number of diffusion experts in the MoDE framework. The analysis was performed on the MS1M dataset, focusing on identification and verification tasks. Two graphs presented in Fig. 6 illustrates the improvement of Top-1 recognition (%) and verification accuracy (Acc) (%). Our findings demonstrate that as the number of experts defined by n increases, there is a consistent upward trend in both the Top-1 and Acc metrics. The improvement appears to stabilize upon reaching a threshold of four to five experts.

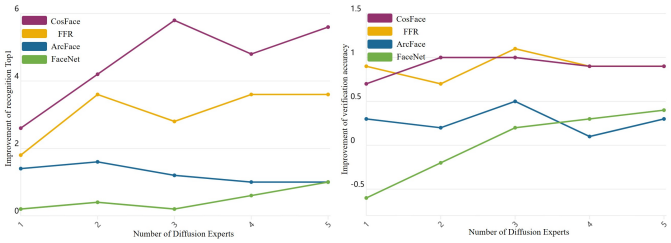

Fig. 6: Hyperparameter analysis of the MoDE method with varying numbers of Diffusion experts.

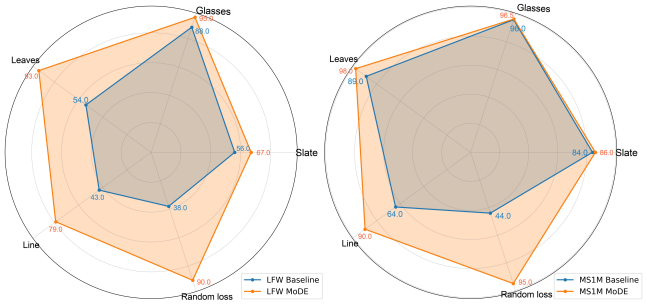

Fig. 7: An illustration of accuracy between different occlusions in LFW and MS1M. The results demonstrate the robustness of the MoDE approach across various occlusions.

Robustness Validation: To assess the efficacy of MoDE on diverse occlusion types, we conducted experiments on the occluded MS1M and LFW datasets, using ArcFace as the baseline. Our results, as presented in Fig. 7, clearly show that MoDE outperforms the baseline method in recognizing occluded faces. Moreover, MoDE demonstrated superior robustness on various types of occlusion and excelled in handling fragmented or randomly dispersed occlusions such as Leaves, Random loss, and Lines.

V. Conclusion

In this paper, we propose an innovative method for occluded face recognition, the Mixtures of Diffusion Experts (MoDE), which employs multiple diffusion experts for reconstruction and utilizes ID-Gate for dynamic integration of expert predictions in the decision space. MoDE is a *plug-and-play* module and exhibits stable and substantial improvements on most face recognition models. Excellent performance on both public and wild datasets with various occlusions demonstrates the robustness of MoDE. Furthermore, our approach presents a novel and promising framework for occluded face recognition, potentially inspiring further research in this domain.

References

[1] Y. Kortli, M. Jridi, A. Al Falou, and M. Atri, "Face recognition systems: A survey," *Sensors*, vol. 20, no. 2, p. 342, 2020.

[2] Y. Sun, Y. Chen, X. Wang, and X. Tang, "Deep learning face representation by joint identification-verification," *Advances in neural information processing systems*, vol. 27, p. n.d., 2014.

[3] J. Zhao, L. Xiong, J. Li, J. Xing, S. Yan, and J. Feng, "3d-aided dual-agent gans for unconstrained face recognition," *IEEE transactions on pattern analysis and machine intelligence*, vol. 41, no. 10, pp. 2380–2394, 2018.

[4] F. Schroff, D. Kalenichenko, and J. Philbin, "Facenet: A unified embedding for face recognition and clustering," in *Proceedings of the IEEE conference on computer vision and pattern recognition*. n.d.: n.d., 2015, pp. 815–823.

[5] Q. Cao, L. Shen, W. Xie, O. M. Parkhi, and A. Zisserman, "Vggface2: A dataset for recognising faces across pose and age," in *2018 13th IEEE international conference on automatic face & gesture recognition (FG 2018)*, IEEE. n.d.: n.d., 2018, pp. 67–74.

[6] H. Wang, Y. Wang, Z. Zhou, X. Ji, D. Gong, J. Zhou, Z. Li, and W. Liu, "Cosface: Large margin cosine loss for deep face recognition," in *Proceedings of the IEEE conference on computer vision and pattern recognition*. n.d.: n.d., 2018, pp. 5265–5274.

[7] J. Deng, J. Guo, N. Xue, and S. Zafeiriou, "Arcface: Additive angular margin loss for deep face recognition," in *Proceedings of the IEEE/CVF conference on computer vision and pattern recognition*. n.d.: n.d., 2019, pp. 4690–4699.

[8] B. Cao, N. Wang, X. Gao, and J. Li, "Asymmetric joint learning for heterogeneous face recognition," in *Proceedings of the AAAI Conference on Artificial Intelligence*, vol. 32, no. 1, 2018.

[9] D. Zeng, R. Veldhuis, and L. Spreeuwers, "A survey of face recognition techniques under occlusion," *IET biometrics*, vol. 10, no. 6, pp. 581–606, 2021.

[10] T. Ahonen, A. Hadid, and M. Pietikäinen, "Face recognition with local binary patterns," in *European conference on computer vision*, Springer. n.d.: n.d., 2004, pp. 469–481.

[11] T. Ahonen, A. Hadid, and M. Pietikainen, "Face description with local binary patterns: Application to face recognition," *IEEE transactions on pattern analysis and machine intelligence*, vol. 28, no. 12, pp. 2037–2041, 2006.

[12] S. Zhao and Z.-p. Hu, "A modular weighted sparse representation based on fisher discriminant and sparse residual for face recognition with occlusion," *Information Processing Letters*, vol. 115, no. 9, pp. 677–683, 2015.

[13] B. Cao, N. Wang, J. Li, and X. Gao, "Data augmentation-based joint learning for heterogeneous face recognition," *IEEE transactions on neural networks and learning systems*, vol. 30, no. 6, pp. 1731–1743, 2018.

[14] Y. Zheng, D. K. Pal, and M. Savvides, "Ring loss: Convex feature normalization for face recognition," in *Proceedings of the IEEE conference on computer vision and pattern recognition*. n.d.: n.d., 2018, pp. 5089–5097.

[15] Y. Wen, K. Zhang, Z. Li, and Y. Qiao, "A discriminative feature learning approach for deep face recognition," in *Computer Vision–ECCV 2016: 14th European Conference, Amsterdam, The Netherlands, October 11–14, 2016, Proceedings, Part VII 14*, Springer. n.d.: n.d., 2016, pp. 499–515.

[16] X. Zhang, Z. Fang, Y. Wen, Z. Li, and Y. Qiao, "Range loss for deep face recognition with long-tailed training data," in *Proceedings of the IEEE International Conference on Computer Vision*. n.d.: n.d., 2017, pp. 5409–5418.

[17] W. Liu, Y. Wen, Z. Yu, and M. Yang, "Large-margin softmax loss for convolutional neural networks," *arXiv preprint arXiv:1612.02295*, vol. n.d., no. n.d., p. n.d., 2016.

[18] Y. Taigman, M. Yang, M. Ranzato, and L. Wolf, "Deepface: Closing the gap to human-level performance in face verification," in *Proceedings of the IEEE conference on computer vision and pattern recognition*. n.d.: n.d., 2014, pp. 1701–1708.

[19] B. Cao, N. Wang, X. Gao, J. Li, and Z. Li, "Multi-margin based decorrelation learning for heterogeneous face recognition," *arXiv preprint arXiv:2005.11945*, 2020.

[20] W. Liu, Y. Wen, Z. Yu, M. Li, B. Raj, and L. Song, "Sphereface: Deep hypersphere embedding for face recognition," in *Proceedings of the IEEE conference on computer vision and pattern recognition*. n.d.: n.d., 2017, pp. 212–220.

[21] L. Wiskott, N. Krüger, N. Kuiger, and C. Von Der Malsburg, "Face recognition by elastic bunch graph matching," *IEEE Transactions on pattern analysis and machine intelligence*, vol. 19, no. 7, pp. 775–779, 1997.

[22] H. Qiu, D. Gong, Z. Li, W. Liu, and D. Tao, "End2end occluded face recognition by masking corrupted features," *IEEE Transactions on Pattern Analysis and Machine Intelligence*, vol. 44, no. 10, pp. 6939–6952, 2021.

[23] R. Weng, J. Lu, and Y.-P. Tan, "Robust point set matching for partial face recognition," *IEEE transactions on image processing*, vol. 25, no. 3, pp. 1163–1176, 2016.

[24] L. He, H. Li, Q. Zhang, and Z. Sun, "Dynamic feature learning for partial face recognition," in *Proceedings of the IEEE conference on computer vision and pattern recognition*. n.d.: n.d., 2018, pp. 7054–7063.

[25] L. Song, D. Gong, Z. Li, C. Liu, and W. Liu, "Occlusion robust face recognition based on mask learning with pairwise differential siamese network," in *Proceedings of the IEEE/CVF International Conference on Computer Vision*. n.d.: n.d., 2019, pp. 773–782.

[26] A. Criminisi, P. Pérez, and K. Toyama, "Region filling and object removal by exemplar-based image inpainting," *IEEE Transactions on image processing*, vol. 13, no. 9, pp. 1200–1212, 2004.

[27] I. Goodfellow, J. Pouget-Abadie, M. Mirza, B. Xu, D. Warde-Farley, S. Ozair, A. Courville, and Y. Bengio, "Generative adversarial networks," *Communications of the ACM*, vol. 63, no. 11, pp. 139–144, 2020.

[28] Z. He, W. Zuo, M. Kan, S. Shan, and X. Chen, "Attgan: Facial attribute editing by only changing what you want," *IEEE transactions on image processing*, vol. 28, no. 11, pp. 5464–5478, 2019.

[29] S. Ge, C. Li, S. Zhao, and D. Zeng, "Occluded face recognition in the wild by identity-diversity inpainting," *IEEE Transactions on Circuits and Systems for Video Technology*, vol. 30, no. 10, pp. 3387–3397, 2020.

[30] B. Cao, N. Wang, J. Li, Q. Hu, and X. Gao, "Face photo-sketch synthesis via full-scale identity supervision," *Pattern Recognition*, vol. 124, p. 108446, 2022.

[31] B. Cao, H. Cao, J. Liu, P. Zhu, C. Zhang, and Q. Hu, "Autoencoder-based collaborative attention gan for multi-modal image synthesis," *IEEE Transactions on Multimedia*, vol. 26, pp. 995–1010, 2023.

[32] B. Cao, Z. Bi, Q. Hu, H. Zhang, N. Wang, X. Gao, and D. Shen, "Autoencoder-driven multimodal collaborative learning for medical image synthesis," *International Journal of Computer Vision*, vol. 131, no. 8, pp. 1995–2014, 2023.

[33] P. Dhariwal and A. Nichol, "Diffusion models beat gans on image synthesis," *Advances in Neural Information Processing Systems*, vol. 34, pp. 8780–8794, 2021.

[34] J. Sohl-Dickstein, E. Weiss, N. Maheswaranathan, and S. Ganguli, "Deep unsupervised learning using nonequilibrium thermodynamics," in *International Conference on Machine Learning*, PMLR. n.d.: n.d., 2015, pp. 2256–2265.

[35] A. Lugmayr, M. Danelljan, A. Romero, F. Yu, R. Timofte, and L. Van Gool, "Repaint: Inpainting using denoising diffusion probabilistic models," in *Proceedings of the IEEE/CVF Conference on Computer Vision and Pattern Recognition*. n.d.: n.d., 2022, pp. 11 461–11 471.

[36] Z. Bi, B. Cao, W. Zuo, and Q. Hu, "Learning a prototype discriminator with rbf for multimodal image synthesis," *IEEE Transactions on Image Processing*, vol. 31, pp. 6664–6678, 2022.

[37] J. Ho, A. Jain, and P. Abbeel, "Denoising diffusion probabilistic models," *Advances in Neural Information Processing Systems*, vol. 33, pp. 6840–6851, 2020.

[38] K. He, X. Zhang, S. Ren, and J. Sun, "Identity mappings in deep residual networks," in *Computer Vision–ECCV 2016: 14th European Conference, Amsterdam, The Netherlands, October 11–14, 2016, Proceedings, Part IV 14*. Springer, 2016, pp. 630–645.

[39] M. I. Jordan and R. A. Jacobs, "Hierarchical mixtures of experts and the em algorithm," *Neural computation*, vol. 6, no. 2, pp. 181–214, 1994.

[40] N. Shazeer, A. Mirhoseini, K. Maziarz, A. Davis, Q. Le, G. Hinton, and J. Dean, "Outrageously large neural networks: The sparsely-gated mixture-of-experts layer," *arXiv preprint arXiv:1701.06538*, vol. n.d., no. n.d., p. n.d., 2017.

[41] S. Hao, C. Chen, Z. Chen, and K.-Y. K. Wong, "A unified framework for masked and mask-free face recognition via feature rectification," in *2022 IEEE International Conference on Image Processing (ICIP)*, IEEE. n.d.: n.d., 2022, pp. 726–730.

[42] H. Phan and A. Nguyen, "Deepface-emd: Re-ranking using patch-wise earth mover's distance improves out-of-distribution face identification," in *Proceedings of the IEEE/CVF Conference on Computer Vision and Pattern Recognition*. n.d.: n.d., 2022, pp. 20 259–20 269.

[43] G. B. Huang, M. Mattar, T. Berg, and E. Learned-Miller, "Labeled faces in the wild: A database forstudying face recognition in unconstrained environments," in *Workshop on faces in'Real-Life'Images: detection, alignment, and recognition*, no. n.d. n.d.: n.d., 2008, p. n.d.

[44] Z. Liu, P. Luo, X. Wang, and X. Tang, "Deep learning face attributes in the wild," in *Proceedings of the IEEE international conference on computer vision*. n.d.: n.d., 2015, pp. 3730–3738.

[45] L. Van der Maaten and G. Hinton, "Visualizing data using t-sne." *Journal of machine learning research*, vol. 9, no. 11, p. n.d., 2008.